Assignment of Downfield Proton Resonances in Purine Nucleoside Phosphorylase•Immucillin-H Complex by Saturation-Transferred NOEs†

Hua Deng,*,‡ Andrzej Lewandowicz,‡ Sean M. Cahill,‡ Richard H. Furneaux,§ Peter C. Tyler,§ Mark E. Girvin,‡ Robert H. Callender,‡ and Vern L. Schramm‡

Department of Biochemistry, Albert Einstein College of Medicine, 1300 Morris Park Avenue, Bronx, New York 10461, and Carbohydrate Chemistry Team, Industrial Research Limited, Lower Hutt, New Zealand

Received October 7, 2003; Revised Manuscript Received November 21, 2003

ABSTRACT: Purine nucleoside phosphorylase (PNP) catalyzes N-ribosidic bond phosphorolysis in 6-oxypurine nucleosides and deoxynucleosides to form purine and α-D-phosphorylated ribosyl products. The transition state has oxacarbenium ion character with partial positive charge near C-1′, ionic stabilization from the nearby phosphate anion, and protonation at N-7 of the purine. Immucillin-H (ImmH) has a protonated N-7 and resembles the transition-state charge distribution when N-4′ is protonated to the cation. It binds tightly to the PNPs with a K_d value 56 pM for human PNP. Previous NMR studies of PNP•ImmH•PO_4 have shown that the N-4′ of bound ImmH is a cation and is postulated to have a significant contribution to its tight binding. Several unassigned downfield proton resonances (>11 ppm) are specific to the PNP•ImmH•PO_4 complex, suggesting the existence of strong hydrogen bonds. In this study, two of the proton resonances in this downfield region have been assigned. Using ^{15}N-7-labeled ImmH, a resonance at 12.5 ppm has been assigned to N-7H. The N-7H resonance is shifted downfield by only ∼1 ppm from its position for ImmH free in aqueous solution, consistent with only a small change in the hydrogen bonding on N-7H upon binding of ImmH to PNP. In contrast, the downfield resonance at 14.9 ppm in the PNP•ImmH•PO_4 complex is assigned to N-1H of ImmH by using saturation-transferred NOE measurements on the PNP•ImmH complex. The ∼4 ppm downfield shift of the N-1H resonance from its position for ImmH free in solution suggests that the hydrogen bonding to the N-1H in the complex has a significant contribution to the binding of ImmH to PNP. The crystal structure shows Glu201 is in a direct hydrogen bond with N-1H and to O-6 through a water bridge. In the complex with 6-thio-ImmH, the N-1H resonance is shifted further downfield by an additional 1.5 ppm to 16.4 ppm, but the relative shift from the value for 6-thio-ImmH free in solution is the same as in the ImmH complex. Since the binding affinity to hPNP for 6-thio-ImmH is decreased 440-fold relative to that for ImmH, the loss in binding energy is primarily due to the hydrogen bond energy loss at the 6-thiol.

Purine nucleoside phosphorylase (PNP)[1] catalyzes the reversible phosphorolysis of the C-1′ to N-9 bond of 6-oxypurine nucleosides and deoxynucleosides (Scheme 1). In humans, the metabolic role is to remove deoxyguanosine that accumulates from DNA turnover and the genetic deficiency of PNP causes a T-cell immunodeficiency due to dGTP accumulation in dividing T-cells (*1*). Inhibition of PNP inhibits the growth of activated T-cells, providing a clinical means to ameliorate T-cell proliferative disorders (*2*). The catalytic acceleration of PNP and phosphoribosyltransferases is achieved through stabilization of an enzyme-bound oxacarbenium ion precursor and strong leaving group interactions to the purine. These features facilitate ribosyl electrophile migration from the purine leaving group to a phosphorus nucleophile immobilized at the catalytic site (*3*). Immucillins incorporate features of the proposed transition states and are potent inhibitors of PNPs from bovine, human, microbial, and malarial sources (*4*−*6*), as well as for human and malarial HGPRTases (*7*−*9*). ImmH (Chart 1) binds with a K_d of 23 pM to bovine PNP and 56 pM to the human enzyme, making it a potent inhibitor of these enzymes.

Features that make ImmH similar to the transition state include an N-4′ substitution for O-4′ in the sugar ring and protonation at N-7 of the 9-deaza ring. Previous NMR studies have shown that ImmH bound to *Mycobacterium tuberculosis* and human PNP is doubly protonated to form the cation at N-4′ and thus mimic the oxocarbenium ion transition state (*10*). Protonation at N-7 results from replacement of nitrogen by carbon in the 9-deazapurine and from the formation of a chemically stable carbon−carbon bond between the C-1′ of

† Supported by Research Grants EB001958 (R.H.C.) and GM41916 (V.L.S.) from the NIH and an award from the New Zealand Office of Science and Technology.

* To whom correspondence should be addressed. Phone: (718) 430-2437. Fax: (718) 430-8565. E-mail: hdeng@aecom.yu.edu.

‡ Albert Einstein College of Medicine.

§ Industrial Research Limited.

[1] Abbreviations: 1 hPNP, human purine nucleoside phosphorylase; hgPRTase, hypoxanthine-guanine pyrophosphoribosyltransferase; ImmH, immucillin-H; ImmHP, immucillin-H 5′-phosphate; S-ImmH, 6-thio-immucillin-H; 9dHX, 9-deazahypoxanthine; STNOE, saturation-transferred nuclear Overhauser effect; STD, saturation transfer difference; HMQC, heteronuclear multiple quantum coherence, HSQC, heteronuclear single quantum coherence: HMBC, heteronuclear multiple bond correlation; DPFGSE, double pulsed field gradient spin−echo; TSP, perdeuterated 3-(trimethylsilyl)propionate sodium salt.

10.1021/bi0358115 CCC: $27.50
Published on Web 01/29/2004

Scheme 1: Reactions Catalyzed by PNP (X = H or OH, Y = H or NH_2)

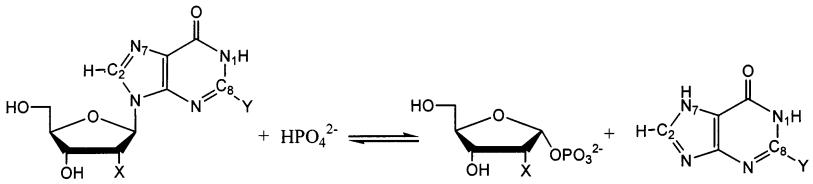

Chart 1: Structure of ImmH, Transition-State Analogue for PNP

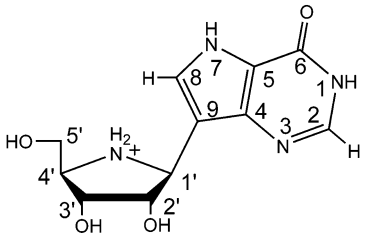

the sugar analogue and the 9-deazapurine moiety. It has been suggested that the elevated pK_a of >10 at N-7 may capture a strong hydrogen bond interaction between the purine and the enzyme that is a feature of the transition state but not the Michaelis complex. This interaction has been identified by NMR and X-ray crystallography in complexes of HGPRT·ImmHP·P_2O_7 (*7*−*9*) and by X-ray crystallography in PNP·ImmH·PO_4 complex (*3*).

The NH resonances for PNP are overlapped in the proton NMR spectrum except for a few unassigned resonances that are in the downfield region of >11 ppm (*11*). However, these downfield resonances are of interest in NMR studies since the corresponding protons are often involved in strong hydrogen-bonding interactions in enzymes (*12*−*16*) and are often at or near the active site. Assignment of these resonances enables one to characterize these hydrogen bonds in the enzyme and enhance our understanding of important enzyme−ligand interactions. As reviewed by Mildvan et al. (*16*), three methods are normally used to assign the downfield proton resonances in the proton NMR spectra of protein−ligand complexes. The most conclusive assignments of downfield resonances have been aided by ^{15}N labeling of the inhibitor using the ^{15}N HMQC type of measurements (see, e.g., refs *7*, *17*, and *18*). Two other methods include mutagenesis of protein (*19*) or alteration of ligand (*20*) and transient or truncated driven NOEs (*12*, *14*, *18*, *21*). Here, all three techniques have been used to assign the downfield resonances in the proton spectrum of the hPNP·ImmH·PO_4 complex. However, it has been found in our enzyme system that the transient and the truncated driven NOE experiments could not yield positive results. The transient NOEs failed because the rapid incoherent exchange process between NH protons of bound and free ligands and the solvent is faster than the coherent transfer process under our experimental conditions. The truncated driven NOEs failed because of the difficulty in assigning the C-2H/C-8H resonances of the bound ligand. Thus, we have developed a variation of these NOE methods, the saturation-transferred NOE (STNOE) method, to aid the assignment of N-1H and N-7H proton resonances found in the downfield NMR spectrum of PNP complexed with immucillin inhibitors.

In this study, both the N-1H and N-7H proton resonances in the human PNP·ImmH·PO_4 complex have been assigned and compared with their values free in solution. To our surprise, the N-7H proton resonance shifts by only ∼1 ppm downfield upon ImmH binding to the complex compared to its value in aqueous solution, suggesting that the hydrogen-bonding change on N-7H is significant but not large. On the other hand, a ∼4 ppm downfield shift of the N-1H proton upon ImmH binding to the complex is observed, consistent with formation of a short, strong hydrogen bond for N-1H in the complex. The results suggest that the major contribution to the binding of the base portion of ImmH is from N-1H rather than from N-7H. Substitution of 6-thio-ImmH for ImmH does not noticeably affect the hydrogen bonding on N-1H, suggesting the 440-fold binding affinity decrease for S-ImmH compared with ImmH in the hPNP complex is primarily due to the loss of hydrogen bonding at C-6═S. Leaving group activation is a major catalytic force for PNP, and the results presented here establish the dominant interactions at C-6═O and N-1 of the purine ring. The relative H bond lengths explain site-directed mutagenesis and inhibitor specificity of mammalian PNPs (*2*, *22*, *23*).

MATERIALS AND METHODS

The compounds ImmH, 6-thio-ImmH (S-ImmH), and [^{15}N-7]ImmH were synthesized as reported (*24*, *25*). Human PNP is a homotrimer of molecular weight 96000 (108000 with the N-terminal extension used in this study). Human purine nucleoside phosphorylase was produced in recombinant form in *E. coli* BL21(DE3) containing the human PNP cDNA in a T7/NT TOPO vector and purified to homogeneity on an affinity resin. Samples of hPNP for NMR were prepared by dialysis of the sample with 0.5 M NaCl at pH 6.0 or 7.0 without buffer, followed by sample concentration with a Centricon-100 to a final concentration of 2 mM monomer, as determined by UV using an extinction coefficient of 30 mM^{-1} cm^{-1} at 280 nm. The concentration of ImmH was determined by UV using an extinction coefficient of 9.5 mM^{-1} cm^{-1} at 261 nm (*4*). The hPNP·ImmH complex was prepared by adjusting the pH of ImmH solutions to 6.0 or 7.0, and lyophilizing appropriate quantities to powder. The proper amount of dry ImmH was added to the concentrated hPNP. The concentration ratio of hPNP to ImmH was 2 mM:10 mM. The ternary complexes of hPNP·(ImmH or S-ImmH)·PO_4 were prepared by adding ImmH and phosphate to the concentrated hPNP solution in 0.5 M NaCl to a final concentration ratio of 2 mM:4 mM:10 mM. The ternary complexes of hPNP·[^{15}N-7]ImmH·PO_4 were prepared by mixing hPNP, inhibitor, and phosphate with a concentration ratio of 1:1.5:5, and the complex was washed three times in a Centricon-100 with 10 volumes of 0.5 M NaCl at pH 6.0, so that the final free inhibitor concentration was less than 0.1% of the protein concentration. D_2O (5%) was added to all NMR samples in aqueous solution to provide deuterium lock.

Solution NMR measurements for proteins, inhibitors, and protein−ligand complexes were obtained on a DRX300 MHz Bruker instrument. 1D proton spectra for samples in aqueous solution were typically collected using 1−1 water suppression using 512 scans, a sweep width of 30 ppm sampled with 16K points, and a recycle delay of 1.5 s. The 1−1 delay was adjusted so that the maximum excitation was at ∼13 ppm, and a 5 Hz line broadening was applied on all presented spectra. Chemical shifts in most 1D spectra were referenced to water resonance (4.7 ppm) unless indicated otherwise. The ^{15}N edited 1D spectra of [^{15}N-7]ImmH were acquired using a 1D version of the HMQC experiment with 7K scans, where all proton pulses were replaced by their 1−1 counterparts (*7*). 2D ^{15}N HMQC spectra for the hPNP·[^{15}N-7]ImmH·PO_4 complex were acquired with the 1−1 version of the HMQC experiments. They were collected with 2K and 16 complex points in t_2 (^{1}H) and t_1 (^{15}N), respectively, with 128 scans per t_1 point and a recycle delay of 1.5 s. The value of $t_{1,max}$ was set to 0.88 ms, and $t_{2,max}$ = 120 ms. An exponential line broadening (10 Hz) was applied to the proton dimension in data processing, and in the ^{15}N dimension, the data were linearly predicted to 64 points and zero filled to 128 points before processing with a cosine bell window function. A sensitivity-enhanced HSQC experiment was used for 2D ^{15}N−^{1}H single or multiple bond correlation spectra of [^{15}N-7]ImmH in DMSO-d_6 or in aqueous solution (with 5% D_2O). In these cases, the $t_{1,max}$ in the ^{15}N dimension was increased to 6.5 ms with 64 data points and 8 scans for each point. The data in the ^{15}N dimension were linearly predicted to 128 points and zero filled to 256 points before processing with a cosine bell window function. The chemical shifts in the proton dimension in the 2D spectra are referenced to that of TSP at 0.0 ppm.

General considerations in performing saturation-transferred NOE (STNOE) experiments, such as determination of the effects of spin diffusion and optimizing experimental conditions, will be discussed in theoretical and experimental detail with relaxation and exchange matrix calculations (Deng et al., submitted for publication). Experimentally, the STNOE measurements were performed on a protein−ligand mixture with excess ligand. This method is based on the principles of truncated driven NOE (*26*) and exchange-transferred NOE (*27*). It is expected to work with protein−ligand systems with the binding constant in the millimolar to submicromolar range, a condition which is similar to that of the exchange-transferred NOE. The implementation of the STNOE measurement is similar to that of the recently published STD measurement (*28*, *29*) except that the transfer period is limited to the initial NOE buildup of the proton resonances of the free ligand and just one protein resonance is selected for saturation. In our implementation, a selective Gaussian-shaped inversion pulse was applied repeatedly on (or off) the proton resonance of interest for a desired time before the observation pulse. A DPFGSE pulse sequence was used for water suppression (*30*). The saturation time was controlled by a loop counter as well as the length of the selective inversion pulse; in a typical measurement, the length of the selective pulse was set to 25 or 30 ms. The acquisition time was set to 0.92 s and recycle delay to 2.5 s. The data were sampled with 16K points with 512 to 1K scans for each spectrum.

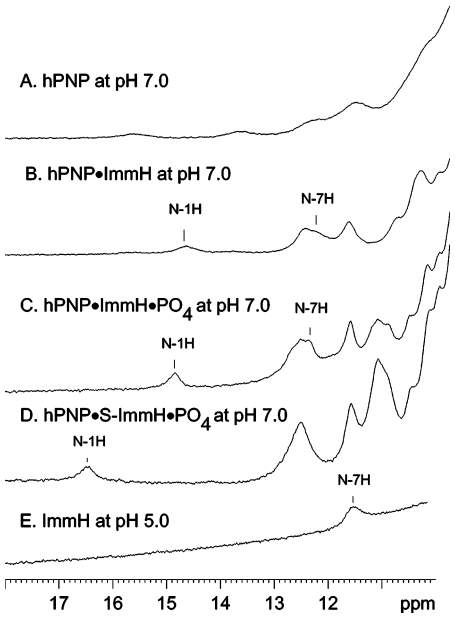

FIGURE 1: Proton spectra of (A) hPNP at 2 mM, (B) hPNP·ImmH complex (2 mM:10 mM), (C) hPNP·ImmH·PO_4 complex (2 mM:4 mM:10 mM), (D) hPNP·S-ImmH·PO_4 complex (2 mM:4 mM:10 mM), and (E) 10 mM ImmH in aqueous solution at pH 5 and 25 °C. All samples were prepared in 95% H_2O + 5% D_2O with 0.5 M NaCl. The pH was 7.0 and the temperature was 40 °C for all protein samples. Other experimental details are described in the Material and Methods.

RESULTS

The downfield region of the proton NMR spectrum of hPNP in aqueous solution (with 5% D_2O) at pH 7.0 and at 40 °C obtained with a 1−1 pulse sequence contains four resonances at 15.7, 13.7, 12.7, and 11.6 ppm (Figure 1A). The intensities of these resonances decrease substantially with decreasing temperature. In the spectrum of hPNP in a binary complex with the inhibitor ImmH under the same conditions, the intensities of the two resonances at 15.7 and 13.7 ppm are greatly reduced and new resonances appear at 14.7 ppm and at ∼12.5 ppm, as a shoulder to the resonance at 12.7 ppm (Figure 1B). The binding of the inhibitor results in the narrowing of the enzyme proton resonances. Bovine PNP is known from H/D exchange to tighten its protein structure in response to ImmH binding (*31*). The proton NMR spectrum of the hPNP·ImmH·PO_4 ternary complex under the same conditions shows the most downfield proton resonance at 14.9 ppm, slightly shifted downfield from that in the binary complex (compare parts B and C of Figure 1). It is reasonable to assume that they are due to the same proton. In addition, approximately three overlapping resonances between 12 and 13 ppm are observed, and several unresolved new resonances between 11 and 12 ppm are also observed. The dissociation constant of ImmH to PNP in the absence of phosphate is approximately 0.44 μM, orders of magnitude looser than that in the presence of the phosphate because of an ionic interaction between bound PO_4 and the iminoribitol cation of bound ImmH. This geometry suggests that the resonances at 14.9 ppm and between 12 and 13 ppm may be related to the interaction between the base portion of bound ImmH while other resonances may be related to the binding of phosphate and/or the iminoribitol group of ImmH. Figure 1D shows the spectrum of the hPNP·S-ImmH·PO_4 complex under the same conditions. The most noticeable change

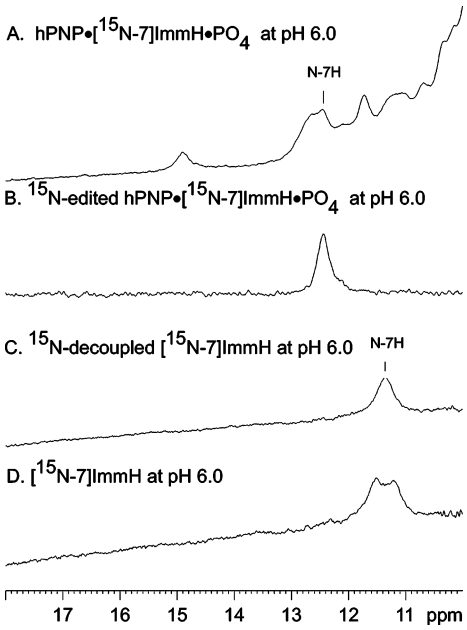

FIGURE 2: Proton spectra of (A) hPNP·[^{15}N-7]ImmH·PO_4 complex (2 mM:2 mM:2 mM) with ^{15}N decoupling during acquisition, (B) the same protein complex with ^{15}N filtering (HMQC), (C) [^{15}N-7]-ImmH in aqueous solution with ^{15}N decoupling during acquisition, and (D) [^{15}N-7]ImmH in aqueous solution without ^{15}N decoupling during acquisition. All samples were prepared in 95% H_2O + 5% D_2O with 0.5 M NaCl. The pH was 6.0 and the temperature was 35 °C for all protein samples. For ImmH solution samples, the pH was 6.0 and temperature was 4 °C.

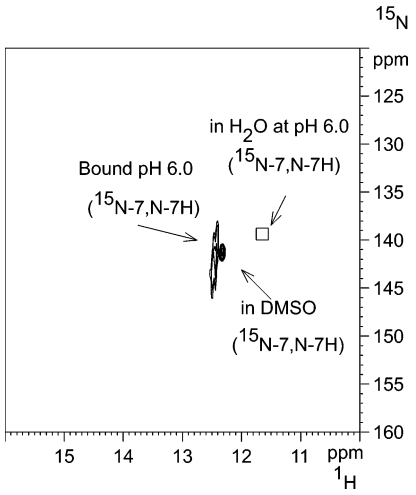

FIGURE 3: ^{15}N−^{1}H correlation spectra of hPNP·[^{15}N-7]ImmH·PO_4 complex at pH 6.0 compared to [^{15}N-7]ImmH in DMSO and in aqueous solution at pH 6.0. The chemical shifts are referenced to that of TSP. Other experimental details are described in the Material and Methods.

compared to the hPNP·ImmH·PO_4 spectrum is the most downfield shifted resonance at 16.4 ppm, suggesting that this resonance is due to a proton near C-6 of (S-)ImmH in the complex. No significant changes were observed in these complexes when the pH was adjusted between 6 and 8. Figure 1E shows the spectrum of ImmH alone in aqueous solution (5% D_2O) at pH 5 and at 25 °C. At this pH, the N-4′ (pK_a 6.9) in ImmH is a doubly protonated cation (*10*). A single resonance at 11.5 ppm is observed in this spectral region. The line width of this resonance increases with increasing temperature and/or increasing pH.

Assignments of the ImmH N-7H resonances in the enzyme complexes and in aqueous solution were achieved using [^{15}N-7]ImmH. The proton spectrum of hPNP·[^{15}N-7]ImmH·PO_4 complex in aqueous solution (5% D_2O), pH 6.0 at 35 °C, with ^{15}N decoupling during acquisition (Figure 2A) was similar to that of the unlabeled ImmH complex obtained under somewhat different conditions (compare Figure 1C). Using a 1D version of the ^{15}N HMQC experiment, the resonance at 12.5 ppm in the hPNP·ImmH·PO_4 complex was identified as the N-7H proton (Figure 2B). The environmental change of the N-7H moiety upon ImmH binding to the enzyme complex was established by comparison of the proton NMR spectrum for the [^{15}N-7]ImmH in aqueous solution with that in the complex. Proton spectra in 95% H_2O + 5% D_2O, pH 6.0 at 4 °C, with and without ^{15}N decoupling during acquisition was used to assign the signal at 11.4 ppm to the N7-H proton (Figure 2C,D). Thus, an about 1 ppm downfield shift of the N-7H proton resonance occurred upon binding of ImmH to hPNP·ImmH·PO_4.

The effect of solvent on the chemical shift of N-7 and N-7H was measured using 2D ^{15}N−^{1}H correlation measurements with [^{15}N-7]ImmH in DMSO, H_2O + 5% D_2O at pH 6, and with the hPNP·[^{15}N-7]ImmH·PO_4 ternary complex at pH 6.0 (Figure 3). Due to the rapid chemical exchange of the N-7H proton with water, the direct measurement in aqueous solution did not yield a 2D spectrum with good signal-to-noise ratio within a reasonable time for ImmH at this pH. Thus, the ^{15}N chemical shift of the N-7 of ImmH in aqueous solution was obtained from a ^{1}H−^{15}N HMBC spectrum in which the N-7 shows a correlation to the C-8H proton. The result of this measurement was combined with the result shown in Figure 2C to yield the predicted resonance (represented by a square) in Figure 3. It can be seen that while the changes of the N-7 and N-7H chemical shifts of ImmH upon binding to the hPNP complex were significant, they do not suggest a strong hydrogen bonding on N-7H in the complex.

Measurements by the STNOE method were used to map other downfield proton resonances from the enzyme-bound inhibitors. By selectively saturating one of the downfield proton resonances observed in the protein−ligand complex, an NOE may be observed on one or more of the free ligand protons through one- or multiple-step spin−spin relaxation (spin diffusion) and then through the exchange between bound and free ligands. Such NOEs should occur when the proton of the bound ligand is spatially close to the proton being saturated, or when the saturation time is long enough. The NOE buildup could be due to either direct spin−spin relaxation or spin diffusion, followed by the exchange between free and bound ligands. The closer this proton is to the one being saturated, the shorter the saturation time needed to observe the NOE on this proton in the free ligand. Thus, by monitoring the NOE buildup of the proton resonance of the free ligands versus the saturation time, one can determine the proximity of this proton to that being saturated. Under favorable conditions, for example, when an internal reference is available, the downfield proton resonance may be assigned.

This method relies on the exchange between bound and free ligands. Since the binding of ImmH in the hPNP·ImmH·PO_4 ternary complex is extremely tight (56 pM), we applied this method to the hPNP·ImmH complex with a concentration ratio of 2 mM:10 mM. The STNOE buildup of the aromatic proton resonances in free ImmH was readily

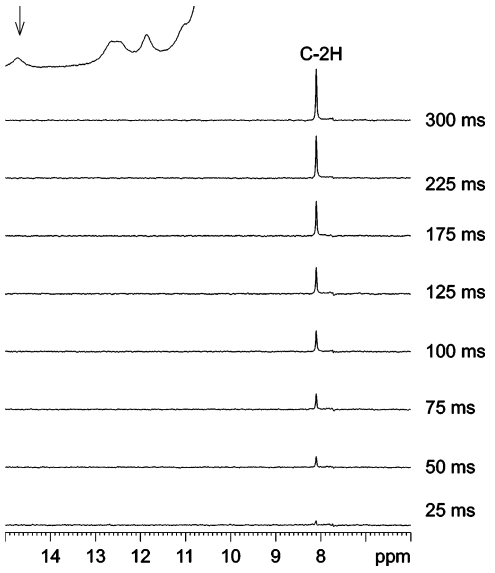

FIGURE 4: STNOE buildup experiments with the hPNP•ImmH complex (2 mM:10mM, pH 7 at 35 °C). The selective pulse was set on resonance at 14.7 ppm (arrow), and the saturation times are indicated next to each curve. Experimental details are described in the Material and Methods.

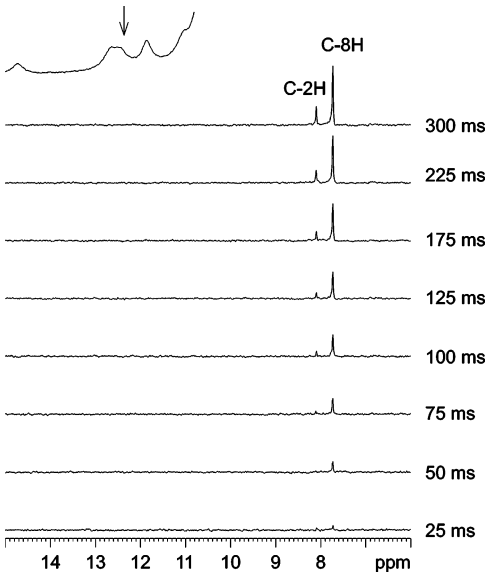

FIGURE 5: STNOE buildup experiments with the hPNP•ImmH complex (2 mM:10mM, pH 7 at 35 °C). The selective pulse was set on resonance at 12.5 ppm (arrow), and the saturation times are indicated next to each curve. Experimental details are described in the Material and Methods.

apparent upon saturation of the resonance at 14.7 ppm in the spectrum of the hPNP•ImmH complex (Figure 4). The top spectrum in Figure 4 is the 1−1 proton spectrum of the hPNP•ImmH complex, and the arrow points to the resonance being saturated. It is obvious that the STNOE on the C-2H resonance increases as the time of saturation on the 14.7 ppm resonance increases, establishing that the 14.7 ppm resonance belongs to a proton that is close to the C-2H of ImmH in the complex but is not close to C-8H.

The broad band between 12 and 13 ppm consists of two nearly overlapping resonances which can be clearly resolved on a 600 MHz spectrometer (data not shown). The STNOE buildup of the free ImmH upon saturation of the resonance at 12.5 ppm (the upfield side of the broad band, known to be from N-7H as shown by the ^{15}N HMQC measurements using [^{15}N-7]ImmH, Figures 2 and 3) is shown in Figure 5. The top proton spectrum is from the hPNP•ImmH complex. The arrow points to the 12.5 ppm resonance being saturated. In this case, both the C-2H and C-8H protons of ImmH showed STNOE buildup with increasing saturation of the N-7H resonance at 12.5 ppm. The STNOE intensity buildup on the C-2H resonance started ∼50 ms later than that on the C-8H and increased at a significantly slower rate. These results indicate qualitatively that the 12.5 ppm resonance belongs to a proton that is closer to the C-8H of ImmH in the complex than to C-2H. Comparing Figures 4 and 5, one can see that the STNOE on C-2H and C-8H appears at about the same saturation time and increases at the same rate with increasing saturation time upon saturation of the resonances at 14.7 and 12.5 ppm, respectively. Thus, the distance between the proton with the resonance at 14.7 ppm and the C2-H should be the same as the distance between the proton with the 12.5 ppm resonance and the C-8H. Since it is known that the 12.5 ppm resonance in the complex is due to N-7H, we conclude that the 14.7 ppm resonance must be due to N-1H.

Our measurement of S-ImmH in DMSO shows that the chemical shift of N-1H in DMSO is ∼1.5 ppm downfield shifted (data not shown) relative to that of N-1H in ImmH in DMSO (Figure 3), which is the same relationship between the 16.4 ppm resonance in the hPNP•S-ImmH•PO_4 complex (Figure 1D) and the 14.9 ppm resonance in the hPNP•ImmH•PO_4 complex (Figure 1C). Therefore, it is reasonable to conclude that the 16.4 and 14.9 ppm resonances are from N-1H of S-ImmH and ImmH, respectively, in the complex.

The observation of an STNOE buildup on C-2H upon saturation of the resonance at 12.5 ppm was puzzling. While it could be argued that N-7H is close enough to C-2H so that an indirect NOE can occur through spin diffusion, it cannot explain why a similar STNOE effect was not observed on C-8H when the resonance at 14.7 ppm was saturated (Figure 4). Several possibilities for this observation are explored in the Discussion.

As a control, similar measurements were made using selective pulses on several other resonances, including the resonances at 12.8 and 11.5 ppm of the hPNP•ImmH complex. No STNOE effect was observed in these cases until the saturation time exceeded ∼350 ms. One of these control measurements, with the selective pulse on the 11.5 ppm resonance (indicated with an arrow), is shown in Figure 6. An STNOE effect on both the C-2H and C-8H resonances started to appear at about the same time when the saturation time reached 360 ms. Spin diffusion pathways within the protein are likely responsible for their appearance in the STNOE experiment. Such results indicate that the resonances at 12.8 and 11.5 ppm belong to protons that are relatively far away from the binding site of the ImmH base. Since resonances at the same chemical shifts are also observed in the apo-hPNP spectrum (Figure 1A), these protons may have structural significance.

DISCUSSION

The immucillins are transition-state analogues of N-ribosyltransferases, and chemical synthesis of these analogues with isotopic labels provides novel spectroscopic probes.

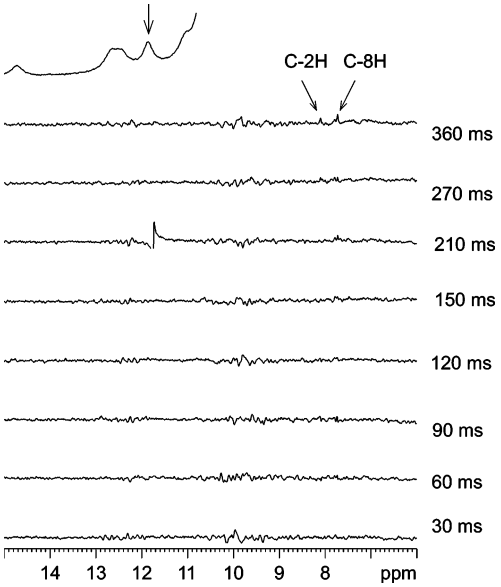

FIGURE 6: STNOE buildup experiments with the hPNP·ImmH complex (2 mM:10mM, pH 7 at 35 °C). The selective pulse was set on resonance at 11.5 ppm (arrow), and the saturation times are indicated next to each curve. Experimental details are described in the Material and Methods.

Transition-state structures for N-ribosyltransferases have been obtained from kinetic isotope effects (KIEs) and computational chemistry (*32*, *33*). The N-ribosyltransferases cleave the C−N bond of nucleosides and nucleotides in dissociative mechanisms that form partially developed oxacarbenium ions at the anomeric carbon of ribose in the transition state. The bond order to the nucleophile at the transition state is minimal, implying that transition-state formation is dominated by protonation of the purine ring to make it a better leaving group. Electrostatic stabilization of the oxacarbenium ion by the nearby phosphate anion at the enzyme active site also assists in forming the transition state. The transition state for bovine PNP is formed when the N-ribosidic bond length has increased by only 0.4 Å, followed by a >1.0 Å translocation of the ribosyl C-1′ toward the enzymatically fixed nucleophile (*33*). This mechanism has been proposed to occur in most N-ribosyltransferases (*34*).

ImmH incorporates distinct features of the transition state including positive charge on the iminoribitol and an elevated pK_a at N-7 of the 9dHX ring. The nitrogen at N-7 is protonated as a consequence of the 9-deaza modification, which also provides chemical stability in the C-1′ to C-9 bond replacing the N-ribosidic bond. These features are missing in the reactant state but are found in the transition state for PNP. The affinity of ImmH for PNP exceeds that of normal substrates by approximately 10^6 in the hPNP·ImmH·PO_4 complex. Complexes of the inhibitors with several PNPs have been characterized by X-ray crystallography. Recent NMR studies have shown that the N-4′ of ImmH is cationic when bound to PNP (*10*), and our current NMR experiments contribute information about the environment of the NH groups of the bound ImmH base.

Hydrogen-Bonding Interaction on N-1H in hPNP·ImmH·PO_4. Our STNOE studies establish that the most downfield resonance of this complex at 14.9 ppm is due to N-1H (Figure 4). Compared with its value in DMSO, the N-1H resonance is downfield shifted by ∼4 ppm, suggesting a relatively short hydrogen bond to N-1H in the complex according to an empirically established correlation between hydrogen-bonding distances and NH/OH proton chemical shift values (*16*, *35*). Several factors that cause a ligand N−H proton chemical shift change in proteins include ring current, local hydrogen bonding and/or long-rang electrostatic interactions, and distortion of the ligand (for a recent treatment of the problem, see Neal et al. (*36*)). The X-ray crystal structure of this complex with bovine PNP reveals that the nearby Tyr188 ring is perpendicular to the 9-deaza ring, with its C−OH bond parallel to the C-2H bond of ImmH. Both N-7H and N-1H of ImmH are in approximately the same plane as this Tyr ring about 5 Å away from the center of the ring (*3*). Thus, the ring current from this Tyr may contribute to the observed downfield shift of the N-1H and N-7H proton resonances. However, the estimated downfield shift of a proton resonance caused by an aromatic ring current more than 4 Å away is expected to be quite small, <0.2 ppm (*37*). Thus, it is reasonable to suggest that the major contribution to the downfield chemical shift change of N-1H/N-7H upon ImmH binding to PNP is due to hydrogen bonding/electrostatic interactions. The hydrogen-bonding distances can also be determined by measurement of H/D fractionation factors (*12*, *17*, *19*, *38*, *39*). Currently, such measurements are under way.

The N-1H resonance is only slightly affected by the binding of phosphate to the enzyme complex even though the binding of ImmH to hPNP is ∼5 orders of magnitude tighter in the presence of phosphate. The N-7H resonance is also insensitive to the binding of phosphate, suggesting that the binding energies from the 9dHX portion remain constant and those from the iminoribitol portion of ImmH increase the total binding energy of ImmH in the PNP·ImmH·PO_4 complex. Previous studies based on the chemical substitutions of ImmH on bovine PNP are consistent with this proposal (*11*). For hPNP, a 6-thio substitution causes a 440-fold decrease of ImmH binding affinity in the ternary complex from 56 pM to 25 nM (our unpublished observation). This is in clear contrast with the bovine PNP, in which the binding affinity of S-ImmH is decreased 82600-fold relative to that of ImmH (*11*). Although the N-1H resonance in the hPNP·S-ImmH·PO_4 complex is 1.5 ppm downfield from that found in the corresponding ImmH complex, the N-1H chemical shift of S-ImmH is also 1.5 ppm downshifted compared with that of ImmH in DMSO (data not shown). Thus, the ∼4 ppm downfield shift of the N-1H proton relative to the values free in solution is induced by the hydrogen bonding in their respective hPNP complexes for both ImmH and S-ImmH. Such results suggest that the N-1H chemical shift difference is due to the difference in the molecular structures of the two inhibitors rather than due to the hydrogen bonding to N-1H in the ImmH and S-ImmH PNP complexes. Thus, the loss of the binding energy in the S-ImmH complex is primarily due to the loss of bonding on C-6═S.

Hydrogen-Bonding Interaction on N-7H in hPNP·ImmH·PO_4. On the basis of the transition-state structure of PNP, a strong hydrogen bond between N-7H and the carbonyl from the carboxamide of Asn243 might be expected. However, the N-7 and N-7H resonances shift downfield by only ∼2 and ∼1 ppm, respectively, compared with their values in aqueous solution (Figure 3). These results establish that the hydrogen bond at N-7H becomes only modestly shorter in

the hPNP·ImmH·PO_4 complex than in unliganded ImmH. The N-7H resonance is known to be sensitive to hydrogen bonding since in structures involving HGPRTase complexed with immucillins, the downfield shift of the N-7H resonances is correlated with the increased binding affinity of the inhibitor, with the most downfield shift found at 14.3 ppm (*7*). The X-ray structure of bovine PNP·ImmH·PO_4 indicates that the hydrogen-bonding distance between N-7 and the side chain carboxamide oxygen of Asn243 is 2.8 Å (±0.2 Å), the same distance as that found in the structure of a similar complex involving HGPRTase (*8*, *9*). However, the proton acceptor in HGPRTase is a carboxyl oxygen of Asp137. The carboxamide oxygen is a weaker hydrogen bond partner with the N-7H in PNP and may explain the reduced hydrogen-bonding energy in hPNP. Transition-state stabilization compares Michaelis and transition states. The Michaelis complex of PNP with inosine shows a distance of 3.3 Å between unprotonated N-7 of inosine and a group that could be the carbonyl or the amino group of Asn243 (*1*, *20*). The weak interaction for substrate and the change of the H bond acceptor/donor nature of N-7 on conversion of substrate to transition state results in a favorable interaction between N-7H of ImmH and the carboxamide oxygen of Asn243 at 2.8 Å. This interaction provides a powerful differential force for transition-state stabilization.

Possibility of a Third Proton Resonance near 12.5 ppm in hPNP·ImmH. There are two resonances between 12 and 13 ppm in the spectrum of the hPNP·ImmH complex (Figure 1B; these become resolved in the spectrum taken with a 600 MHz spectrometer, data not shown). When the downfield side of the 12.5 ppm resonance is being saturated, no STNOE is observed (the same as shown in Figure 6). However, when the upfield side of the 12.5 ppm resonance is being saturated, an STNOE effect is observed not only on C-8H but also on C-2H of ImmH (Figure 5). The STNOE effect on C-2H starts to appear 50 ms later and with a slower rate of increase than that on C-8H. This STNOE effect on C-2H is not likely due to direct spin−spin relaxation between N-7H and C-2H since they are about 6 Å apart. It cannot be due to spin diffusion through N-1H since if that is the case, a similar STNOE effect would be observed on C-8H when N-1H is being saturated, which is not observed (Figure 4). The possibility that the base of ImmH flips during binding in the hPNP·ImmH complex can also be excluded on the basis of the same argument. One possibility is that the NOE from N-7H to C-2H is mediated by protons located adjacent to the 9dHX ring. For example, the NH from Gly122 may be part of this pathway. Another possibility is that a proton whose resonance is near 12.5 ppm is responsible for this observation. Clearly, more studies are required to investigate these possibilities.

Effect of Phosphate Binding to the hPNP·ImmH Complex. Crystallographic evidence establishes that the active site in PNP is closed during catalysis by a flap that opens to bind substrates (*2*, *11*). When the flap is tightly sealed, new contacts form between the ligand and protein residues within the catalytic site (*8*, *9*). Structural studies of ImmH and substrates bound to bovine PNP are particularly compelling in that six new H bonds form when PNP·inosine·SO_4 is compared to PNP·ImmH·PO_4 and nine H bonds relax when PNP·ImmH·PO_4 is compared to product complexes. The data presented here show that the charged N-4′ of ImmH and phosphate ion are factors that drive this hydrogen-bonding rearrangement during the tight-binding conformational change, as shown by the appearance of new downfield proton resonances upon addition of phosphate to the hPNP·ImmH binary complex (Figure 1). Molecular dynamic simulations of nucleoside hydrolase (a related purine N-ribosyltransferase) with an iminoribitol transition-state analogue inhibitor bound to the active site indicate that the active site becomes more organized and corresponding protein motions decrease when the transition-state characteristics of the inhibitor are introduced into the simulation (*40*).

Chart 2: Active Site Contacts between Bovine PNP and Catalytic Site Ligands in the Michaelis Analogue Complex of PNP·Inosine·SO_4 and the Complex of PNP·ImmH·PO_4 As Determined in 1.5 Å X-ray Crystal Structures (*3*)[a]

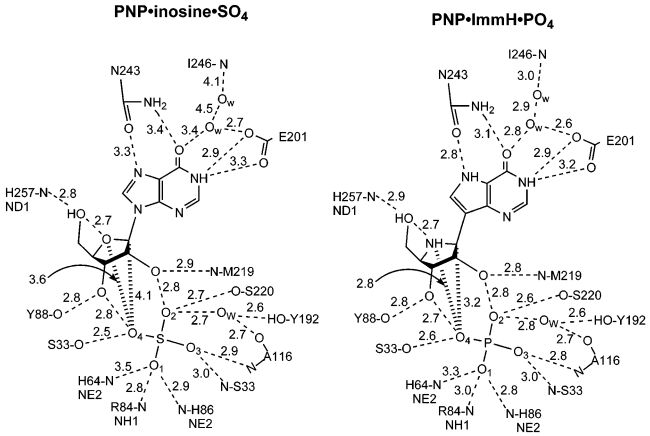

[a] Distances are in angstroms (error ∼0.2 Å). Human PNP is 82% identical with bovine PNP, and all active site residues are conserved.

Conclusions. The interaction between hPNP and 9dHX in the PNP·ImmH·PO_4 complex is characterized by three hydrogen bonds. The 2.8 Å H bond from the carbonyl carboxamide of Asn243 to N-7H (Chart 2) forms as a result of the elevated pK_a and protonation at N-7 of inosine known to occur at the transition state. The interaction causes a chemical shift of ∼1 ppm downfield to 12.5 ppm. Since the interaction between N-7 and the Asn243 carboxamide is repulsive for the inosine complex, the shift to 12.5 ppm indicates the formation of a favorable H bond, a stabilizing force in the complex with the transition-state analogue. The exocyclic O-6 of ImmH accepts a H bond from a water bridge to Glu201, and this shortens from 3.4 Å in the Michaelis complex to 2.8 Å in the complex PNP·ImmH·PO_4 to form a second favorable H bond interaction. Glu201 forms a 2.8 Å H bond to N-1H, giving rise to the most downfield shifted resonance for the interaction in the complex at 14.9 ppm. This interaction anchors the purine ring and is equivalent in the Michaelis complex and the PNP·ImmH·PO_4 complex. Together these interactions are estimated to contribute 10 kcal/mol toward forward catalysis by leaving group activation. Interactions at N-7H and O-6 are specific to the formation of the transition state, while that at N-1H serves to anchor the substrate.

REFERENCES

1. Stoeckler, J. D. (1984) in *Developments in Cancer Chemotherapy* (Glazer, R. J., Ed.) pp 35−60, CRC Press Inc., Boca Raton, FL.
2. Bzowska, A., Kulikowska, E., and Shugar, D. (2000) Purine nucleoside phosphorylases: properties, functions, and clinical aspects, *Pharmacology Ther. 88*, 349−425.

3. Fedorov, A., Shi, W., Kicska, G., Fedorov, E., Tyler, P. C., Furneaux, R. H., Hanson, J. C., Gainsford, G. J., Larese, J. Z., Schramm, V. L., and Almo, S. C. (2001) Transition state structure of purine nucleoside phosphorylase and principles of atomic motion in enzymatic catalysis, *Biochemistry 40*, 853−60.
4. Miles, R. W., Tyler, P. C., Furneaux, R. H., Bagdassarian, C. K., and Schramm, V. L. (1998) One-third-the-sites transition-state inhibitors for purine nucleoside phosphorylase, *Biochemistry 37*, 8615−21.
5. Kicska, G. A., Tyler, P. C., Evans, G. B., Furneaux, R. H., Schramm, V. L., and Kim, K. (2002) Purine-less death in Plasmodium falciparum induced by immucillin-H, a transition state analogue of purine nucleoside phosphorylase, *J. Biol. Chem. 277*, 3226−31.
6. Kicska, G. A., Tyler, P. C., Evans, G. B., Furneaux, R. H., Kim, K., and Schramm, V. L. (2002) Transition state analogue inhibitors of purine nucleoside phosphorylase from Plasmodium falciparum, *J. Biol. Chem. 277*, 3219−25.
7. Li, C. M., Tyler, P. C., Furneaux, R. H., Kicska, G., Xu, Y., Grubmeyer, C., Girvin, M. E., and Schramm, V. L. (1999) Transition-state analogs as inhibitors of human and malarial hypoxanthine-guanine phosphoribosyltransferases, *Nat. Struct. Biol. 6*, 582−7.
8. Shi, W., Li, C. M., Tyler, P. C., Furneaux, R. H., Cahill, S. M., Girvin, M. E., Grubmeyer, C., Schramm, V. L., and Almo, S. C. (1999) The 2.0 A structure of malarial purine phosphoribosyltransferase in complex with a transition-state analogue inhibitor, *Biochemistry 38*, 9872−80.
9. Shi, W., Li, C. M., Tyler, P. C., Furneaux, R. H., Grubmeyer, C., Schramm, V. L., and Almo, S. C. (1999) The 2.0 A structure of human hypoxanthine-guanine phosphoribosyltransferase in complex with a transition-state analog inhibitor, *Nat. Struct. Biol. 6*, 588−93.
10. Sauve, A. A., Cahill, S. M., Zech, S. G., Basso, L. A., Lewandowicz, A., Santos, D. S., Grubmeyer, C., Evans, G. B., Furneaux, R. H., Tyler, P. C., McDermott, A., Girvin, M. E., and Schramm, V. L. (2003) Ionic states of substrates and transition state analogues at the catalytic sites of N-ribosyltransferases, *Biochemistry 42*, 5694−705.
11. Kicska, G. A., Tyler, P. C., Evans, G. B., Furneaux, R. H., Shi, W., Fedorov, A., Lewandowicz, A., Cahill, S. M., Almo, S. C., and Schramm, V. L. (2002) Atomic dissection of the hydrogen bond network for transition-state analogue binding to purine nucleoside phosphorylase, *Biochemistry 41*, 14489−98.
12. Lin, J., Westler, W. M., Cleland, W. W., Markley, J. L., and Frey, P. A. (1998) Fractionation factors and activation energies for exchange of the low barrier hydrogen bonding proton in peptidyl trifluoromethyl ketone complexes of chymotrypsin, *Proc. Natl. Acad. Sci. U.S.A. 95*, 14664−8.
13. Frey, P. A., Whitt, S. A., and Tobin, J. B. (1994) A low-barrier hydrogen bond in the catalytic triad of serine proteases, *Science 264*, 1927−30 (comment).
14. Markley, J. L., and Westler, W. M. (1996) Protonation-state dependence of hydrogen bond strengths and exchange rates in a serine protease catalytic triad: bovine chymotrypsinogen A, *Biochemistry 35*, 11092−7.
15. Gerlt, J. A., Kreevoy, M. M., Cleland, W., and Frey, P. A. (1997) Understanding enzymic catalysis: the importance of short, strong hydrogen bonds, *Chem. Biol. 4*, 259−67.
16. Mildvan, A. S., Harris, T. K., and Abeygunawardana, C. (1999) Nuclear magnetic resonance methods for the detection and study of low-barrier hydrogen bonds on enzymes, *Methods Enzymol. 308*, 219−45.
17. Halkides, C. J., Wu, Y. Q., and Murray, C. J. (1996) A low-barrier hydrogen bond in subtilisin: 1H and 15N NMR studies with peptidyl trifluoromethyl ketones, *Biochemistry 35*, 15941−8.
18. Harris, T. K., Abeygunawardana, C., and Mildvan, A. S. (1997) NMR studies of the role of hydrogen bonding in the mechanism of triosephosphate isomerase, *Biochemistry 36*, 14661−75.
19. Zhao, Q., Abeygunawardana, C., Gittis, A. G., and Mildvan, A. S. (1997) Hydrogen bonding at the active site of delta 5−3-ketosteroid isomerase, *Biochemistry 36*, 14616−26.
20. Kintanar, A., Metzler, C. M., Metzler, D. E., and Scott, R. D. (1991) NMR observation of exchangeable protons of pyridoxal phosphate and histidine residues in cytosolic aspartate aminotransferase, *J. Biol. Chem. 266*, 17222−9.
21. Metzler, D. E., Metzler, C. M., Mollova, E. T., Scott, R. D., Tanase, S., Kogo, K., Higaki, T., and Morino, Y. (1994) NMR studies of 1H resonances in the 10−18-ppm range for cytosolic aspartate aminotransferase, *J. Biol. Chem. 269*, 28017−26.
22. Erion, M. D., Takabayashi, K., Smith, H. B., Kessi, J., Wagner, S., Honger, S., Shames, S. L., and Ealick, S. E. (1997) Purine nucleoside phosphorylase. 1. Structure−function studies, *Biochemistry 36*, 11725−34.
23. Stoeckler, J. D., Poirot, A. F., Smith, R. M., Parks, R. E., Jr., Ealick, S. E., Takabayashi, K., and Erion, M. D. (1997) Purine nucleoside phosphorylase. 3. Reversal of purine base specificity by site-directed mutagenesis, *Biochemistry 36*, 11749−56.
24. Evans, G. B., Furneaux, R. H., Gainsford, G. J., Hanson, J. C., Kicska, G. A., Sauve, A. A., Schramm, V. L., and Tyler, P. C. (2003) 8-Aza-immucillins as transition-state analogue inhibitors of purine nucleoside phosphorylase and nucleoside hydrolases, *J. Med. Chem. 46*, 155−60.
25. Evans, G. B., Furneaux, R. H., Hutchison, T. L., Kezar, H. S., Morris, P. E., Jr., Schramm, V. L., and Tyler, P. C. (2001) Addition of lithiated 9-deazapurine derivatives to a carbohydrate cyclic imine: convergent synthesis of the aza-C-nucleoside immucillins, *J. Org. Chem. 66*, 5723−30.
26. Wagner, G., and Wüthrich, K. (1979) Truncated Driven Nuclear Overhauser Effect(TOE). A New Technique for Studies of Selective ^{1}H-^{1}H Overhauser Effects in the presence of spin diffusion, *J. Magn. Reson. 33*, 675−680.
27. Clore, G. M., and Gronenborn, A. M. (1982) Theory and application of the transferred nuclear overhauser effect to the study of the conformations of small ligands bound to proteins, *J. Magn. Reson. 48*, 402−417.
28. Haselhorst, T., Espinosa, J. F., Jimenez-Barbero, J., Sokolowski, T., Kosma, P., Brade, H., Brade, L., and Peters, T. (1999) NMR experiments reveal distinct antibody-bound conformations of a synthetic disaccharide representing a general structural element of bacterial lipopolysaccharide epitopes, *Biochemistry 38*, 6449−59.
29. Mayer, M., and Meyer, B. (1999) Characterization of ligand binding by saturation transfer difference NMR spectroscopy, *Angew. Chem. Int. Ed. 38*, 1784−1788.
30. Hwang, T. L., and Shaka, A. J. (1995) Water suppression that works. Excitation sculpting using arbitrary wave-forms and pulsed-field gradients, *J. Magn. Reson., A 112*, 275−279.
31. Wang, F., Miles, R. W., Kicska, G., Nieves, E., Schramm, V. L., and Angeletti, R. H. (2000) Immucillin-H binding to purine nucleoside phosphorylase reduces dynamic solvent exchange, *Protein Sci. 9*, 1660−8.
32. Kline, P. C., and Schramm, V. L. (1993) Purine nucleoside phosphorylase. Catalytic mechanism and transition-state analysis of the arsenolysis reaction, *Biochemistry 32*, 13212−9.
33. Kline, P. C., and Schramm, V. L. (1995) Pre-steady-state transition-state analysis of the hydrolytic reaction catalyzed by purine nucleoside phosphorylase, *Biochemistry 34*, 1153−62.
34. Schramm, V. L., and Shi, W. (2001) Atomic motion in enzymatic reaction coordinates, *Curr. Opin. Struct. Biol. 11*, 657−65.
35. Wei, Y., and McDermott, A. E. (1999) in *Modeling NMR Chemical Shifts: gaining insights into structure and environment* (Facelli, J. C., and deDios, A. C., Eds.) pp 177−193, Oxford University Press, Oxford, U.K..
36. Neal, S., Nip, A. M., Zhang, H., and Wishart, D. S. (2003) Rapid and accurate calculation of protein 1H, 13C and 15N chemical shifts, *J. Biomol. NMR 26*, 215−40.
37. Johnson, C. E., and Bovey, F. A. (1958) Calculation of nuclear magnetic resonance spectra of aromatic hydrocarbon, *J. Chem. Phys. 29*, 1012−1014.
38. Loh, S. N., and Markley, J. L. (1994) Hydrogen bonding in proteins as studied by amide hydrogen D/H fractionation factors: application to staphylococcal nuclease, *Biochemistry 33*, 1029−36.
39. Kreevoy, M. M., and Liang, T. M. (1980) Structures and isotopic fractionation factors of complexes, A1HA2-, *J. Am. Chem. Soc. 102*, 3315−3322.
40. Mazumder, D., Kahn, K., and Bruice, T. C. (2002) Computer simulations of trypanosomal nucleoside hydrolase: determination of the protonation state of the bound transition-state analogue, *J. Am. Chem. Soc. 124*, 8825−33.

BI0358115